

## METHODS OF CRYOSPHERIC RESEARCH

SHALLOW-DEPTH TRANSIENT ELECTROMAGNETIC SOUNDINGS  
FOR IDENTIFICATION OF GAS-HYDRATE ACCUMULATIONS  
IN THE CRYOLITHOZONE OF THE NORTHERN REGIONS OF WESTERN SIBERIAE.V. Murzina<sup>1,3</sup>, A.V. Pospeev<sup>1,2</sup>, I.V. Buddo<sup>1–3</sup>, M.V. Sharlov<sup>3</sup>,  
I.K. Seminskiy<sup>1,3</sup>, N.V. Misyurkeeva<sup>1,3</sup>, I.A. Shelohov<sup>1,3</sup><sup>1</sup> Institute of the Earth's Crust, Siberian Branch of the Russian Academy of Sciences, Lermontova str. 128, Irkutsk, 664033 Russia<sup>2</sup> Irkutsk National Research Technical University, Lermontova str. 83, Irkutsk, 664074 Russia<sup>3</sup> SIGMA-GEO LLC, Zvezdinskaya str. 6, Irkutsk, 664039 Russia; [mkv@sigma-geo.ru](mailto:mkv@sigma-geo.ru)

The territory of the north of Western Siberia is known as one of the promising regions of the Russian Arctic in terms of reserves of alternative fuel sources, in particular, gas hydrates. According to the results of interpretation of the data of 3D areal near-field transient electromagnetic sounding (NTES) in the permafrost zone, performed in Nadym district of the Yamalo-Nenets Autonomous okrug at depths of 100–220 m, geoelectric anomalies of increased electrical resistivity values were revealed, accompanied by the manifestation of double induced polarization. The authors associate the mentioned anomalies with the possible accumulations of gas hydrates in the permafrost thickness. To justify the applicability of the sounding method by the formation of the field in the near zone in a shallow modification for mapping subpermafrost geoelectric anomalies in the permafrost zone, a description of a mathematical experiment is presented. The experiment is based on empirical electromagnetic data. As a result of mathematical modeling, it is shown that the use of electromagnetic soundings by the formation of the field in the near zone makes it possible to estimate the conductivity and polarizability of the upper part of the section of the study area and to identify anomalies in the permafrost zone, which are probably associated with hydrate-bearing deposits.

**Keywords:** frozen ground, permafrost zone, gas hydrate, near-field transient electromagnetic sounding (NTES), double-induced polarization, electrical resistivity

## INTRODUCTION

In recent decades, an active search and exploration of hydrocarbon deposits has been carried out in the Russian Arctic. A significant role is played by electromagnetic studies, including near-field transient electromagnetic sounding (NTES) aimed at studying the reservoir properties of the target intervals in both the upper and lower stages of the geological section [Van'yan, 1965]. The most important feature of the north of Western Siberia is the widespread distribution of permafrost—the upper layer of the earth's crust characterized by subzero temperatures of soils and rocks, regardless of the phase state of water in it [Shvetsov, 1955; Romanovsky, 1993]. Permafrost includes frozen (with ice), dry cryotic, and cryotic rocks. Cryotic rocks are saline or saturated with saline waters and brines with temperatures below 0 °C.

Another promising object of the study is represented by gas hydrates associated with permafrost. Gas hydrates are ice-like crystalline compounds that form at certain temperatures and pressures from water molecules and low-molecular-weight gas (CH<sub>4</sub>, C<sub>2</sub>H<sub>6</sub>, CO<sub>2</sub>, N<sub>2</sub>, etc.) [Istomin and Yakushev, 1992].

The search, exploration, and development of hydrate-bearing accumulations in the Russian Arctic is limited by the inaccessibility of the region and the lack of a well-developed set of geophysical methods comparable in efficiency to marine research. In particular, marine electrical exploration CSEM (controlled source electromagnetic method) in combination with seismic exploration by the common depth point method (CDP) has become popular abroad to search for deposits of gas hydrates in the shelf zone [Vorob'ev and Malyukov, 2009]. A prerequisite for the successful application of shallow near-field transient electromagnetic sounding (shallow NTES) for solving geocryological problems is the differentiation of the geoelectric characteristics of sedimentary rocks depending on their moisture content and ice content [Stogniy, 2003; Kozhevnikov et al., 2014; Ageev, 2019]. The efficiency of the shallow NTES method for studying both the upper part of the section and the deep (up to 3–4 km) layers in the geological conditions of Western Siberia is also reflected in [Buddo et al., 2017, 2018, 2021; Sharlov et al., 2017; Misyurkeeva et al., 2017, 2019, 2020, 2021; Shelokhov et al., 2018;

*Dolgikh et al., 2019; Rybalchenko et al., 2020*]. However, there is practically no confirmation of the results of interpretation of geophysical data indicating the detection of gas hydrate accumulations in the permafrost by direct field methods (drilling of the wells).

In this article, the authors present and discuss the results of the work carried out by the shallow NTES method on the Tazovsky Peninsula (Nadym district). According to the results of electrical surveys, there are high-resistivity anomalies of specific electrical resistance (SER) accompanied by anomalies of doubled induced polarization (DIP) in the permafrost [*Murzina et al., 2016; Misyurkeeva et al., 2017, 2021*]. Geoelectric structures of this kind were also found by other researchers [*Kozhevnikov and Antonov, 2010; Afanasenkov et al., 2015*] based on the results of electromagnetic survey in the Russian Arctic.

### ON GAS HYDRATES IN PERMAFROST OF THE NORTH OF WESTERN SIBERIA

Though most of the gas hydrate deposits discovered to date are confined to sea areas, the first indication of the existence of continental gas hydrate deposits in the permafrost zone were discovered in the early 1950s in Eastern Siberia [*Chersky and Tsarev, 1973*]. Large accumulations of gas hydrates are known in frozen deposits of the Mackenzie River delta in Canada and in northern Alaska within large oil and gas fields [*Aregbe, 2017; Uchida et al., 2000*]. The existence of layers with gas hydrates in permafrost of northern areas of Western Siberia identified mainly by indirect evidence within the Messoyakha, Yamburg, and Bovanenkovo fields was mentioned in a number of recent studies [*Yakushev and Chuvilin, 2000; Chuvilin et al., 2000, 2007; Yakushev et al., 2003; Yakushev, 2009; Leonov, 2010*].

When analyzing the conditions for the existence of gas hydrate formations in the north of Western Siberia, many researchers use such concepts as zones of stability [*Istomin and Yakushev, 1992*] and metastability of gas hydrates [*Perlova, 2001; Yakushev et al., 2003*]. The term “gas hydrate stability zone” (GHSZ) is currently understood as “a part of the lithosphere and hydrosphere of the Earth, the thermobaric and geochemical regimes of which correspond to the conditions for the stable existence of natural gas hydrates of a certain composition” [*Istomin and Yakushev, 1992, p. 175*].

The gas hydrate metastability zone (GHMZ) is a part of the permafrost section above the top of GHSZ, where the temperature regime of the rocks suggests the possibility of self-preservation of gas hydrates at subzero temperatures [*Perlova, 2001*]. In particular, according to the latest data, gas hydrates can form and exist for a long time in frozen sandy sediments with a low degree of salinity [*Chuvilin et al., 2018, 2019*].

Not much is known about the distribution of gas hydrates within terrestrial paleobasins. Thus, in the Mackenzie River delta, their presence in is possible in permafrost areas, because the GHSZ on land is only formed in association with permafrost [*Uchida, et al., 2000*]. Favorable conditions for the formation of subpermafrost and intrapermafrost gas hydrate deposits exist in the northern part of the West Siberian basin with a continuous permafrost of 200–400 m in thickness [*Ershov, 1989; Leonov, 2010*].

As a rule, large accumulations of gases in the clathrate form are confined to areas of oil and gas fields [*Yakushev et al., 2003; Chuvilin et al., 2007; Yakushev, 2009*] and may consist of not only catagenic gas but also biogenic gas formed during the microbial decomposition of organic matter in sedimentary deposits [*Yakushev and Chuvilin, 2000; Yakushev, 2009; Leonov, 2010*]. Most often, such accumulations are located in the GHSZ, but there are exceptions, in particular, the Yamburg gas condensate field on the Tazovsky Peninsula, 60 km north of the study area. The presence of metastable gas hydrates in the permafrost strata was noted here based on active gas manifestations and the determination of gas content in core samples at depths of 70–120 m [*Istomin and Yakushev, 1992*].

On the example of the Bovanenkovo field, V.L. Bondarev showed the presence of traces of fluid migration in the form of gas shows in the intervals of supra-Cenomanian deposits. Most of the gas shows are confined to the interval of 38–120 m [*Bondarev et al., 2008*]. Methane in the composition of gases is of predominantly biogenic origin. In some cases, the <sup>13</sup>C isotope is present in the gases, which may indicate the presence of some amounts of epigenetic (migratory) gases in their composition [*Bondarev et al., 2004*].

In addition, heaving mounds (bulgunnyakhs) are widespread in the north of Western Siberia in the basins of drained thermokarst lakes (khasyryes). Some heaving mounds are considered traces of hydrovolcanic processes [*Nezhdanov et al., 2011; Bogoyavlensky et al., 2019*]. This indicates the possibility of methane entering with the upward flows of formation waters; this gas may be a “building material” for the formation of subpermafrost accumulations of gas hydrates.

From the foregoing, it follows that the existence of stable gas hydrate formations associated with a thick permafrost and metastable relict accumulations of gas hydrates associated with incompletely thawed frozen strata of the past is possible in the north of Western Siberia. Metastable gas hydrates are not only a potential source of hydrocarbons located close to the surface; they are also an extremely unstable and explosive substance [*Perlova et al., 2017*], the position of which in the section must be taken into account when drilling and spudding deep wells.

### Mapping of sediments with possible hydrate content according to data of shallow near-field transient electromagnetic sounding in the north of Western Siberia

The studied, data from which are presented in this article and form the basis for further synthetic modeling, is located in the Tazovsky Peninsula, on the interfluvium between the Khadutte and Tabyakha rivers in the upper reaches, on the schematic map of permafrost zoning [Baulin *et al.*, 1967], it belongs to the northern zone, subzone of predominantly epigenetically frozen deposits (Fig. 1). Alluvial, lacustrine-alluvial, and alluvial-estuary deposits of river terraces are epigenetically frozen; their freezing occurred from top to bottom after sedimentation.

The study area is located in the area of disjunct occurrence of modern and relict frozen strata separated by taliks. The total thickness of the cryogenic strata reaches 400 m and more. There are also numerous open and closed taliks under riverbeds and lakes, as well as areas of a sharp increase in the thickness of frozen strata [Baulin *et al.*, 1967; Shpolyanskaya, 1981].

The measurements were carried out using a Fast-Snap digital telemetry station for shallow-depth surveys over a dense network of observations (100 ob-

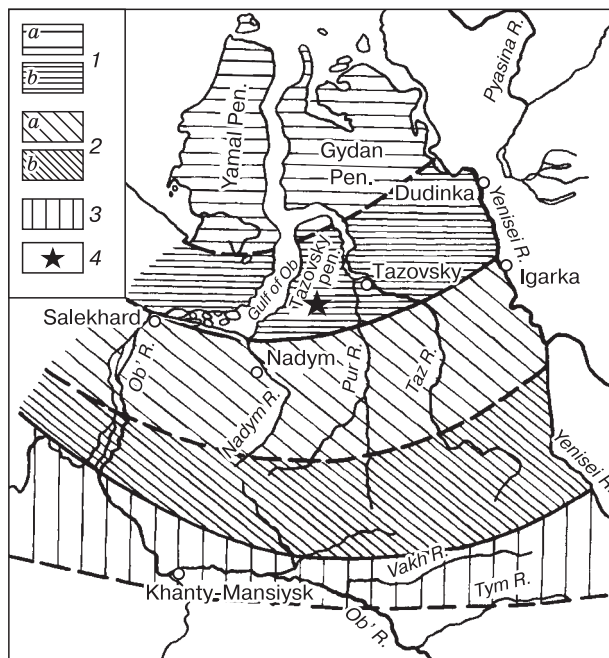


Fig. 1. Schematic map of permafrost zones and sub-zones [Baulin *et al.*, 1967].

1 – northern zone (a, subzone of polygenetically frozen sediments; b, subzone of predominantly epigenetically frozen sediments); 2 – central zone (a, subzone of frozen mineral soils and peat bogs; b, subzone of frozen peat bogs); 3 – southern zone of deep-lying relict frozen strata; 4 – area of field work with shallow-depth NTES.

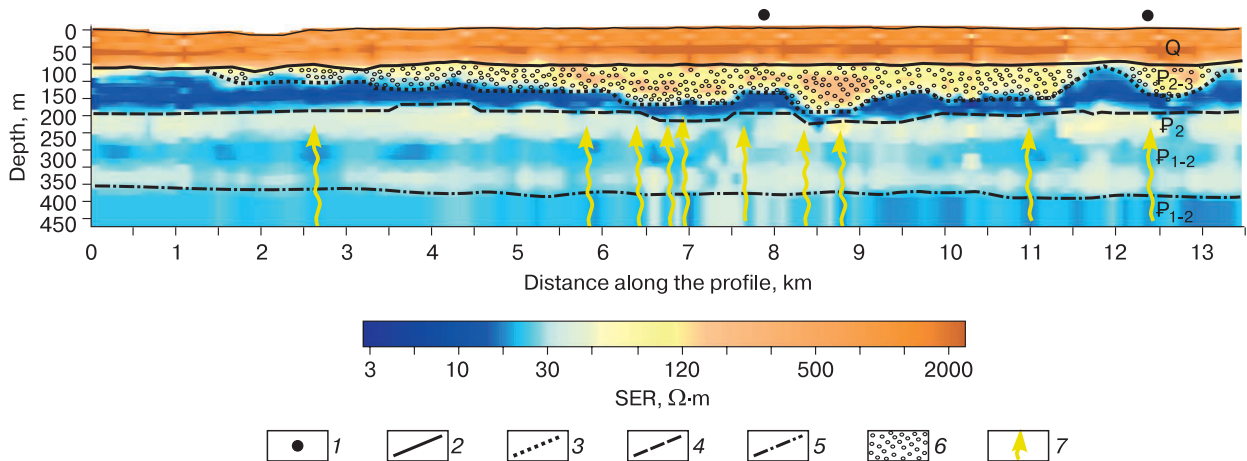
servations points per 1 km<sup>2</sup>). A coaxial array with a 100 × 100 m generator loop and two 10 × 10 m receiving loops at a distance of 0 and 100 m from the array center was used as a probing array.

Figure 2 displays a section along the 13,500-m-long shallow NTES profile oriented from south to north. The upper layer of modern permafrost with increased electrical resistivity values (from 500 to 2000 Ω·m) reaches a depth of about 80–100 meters. This layer is characterized by a sharp increase in resistivity values compared to the underlying strata. It is represented by lacustrine-alluvial, alluvial-marine, and glacial-marine deposits of the Quaternary age [Shatsky, 1978]. Taking into account the geocryological conditions of the study area [Ershov, 1989], the high-resistivity horizon identified in the upper part of the section is associated with the area of permafrost development and is characterized by the increased ice content and temperatures of about –5 °C.

On the profile built according to the shallow NTES data (Fig. 2), within intervals of 2.0–11.6, 12.2–13.1 km, the modern layer of frozen rocks (resistivity 500–2000 Ω·m) is underlain by a heterogeneous layer with the lower boundary in the form of high-resistivity “pockets”. The resistivity of rocks in this interval decreases to 20–80 Ω·m with local peaks up to 150–300 Ω·m. The thickness of this layer is also quite variable, from 50 to 160 m. This interval is mainly represented by the Korlikovskaya sequence (Oligocene) of whitish and light gray sands, poorly sorted, with lenses of gravelstones. The abundance of kaolin in the form of nest filler, lenticular layers, and pellets is typical [Shatsky, 1978]. On the graph of temperature distribution over depth [Ershov, 1989], the permafrost temperature in this layer (at depths from 100 to 200 m) increases with depth from –4 to –2 °C. A significant decrease in resistivity relative to the overlying high-resistivity horizon can also be associated with a decrease in the ice content with depth.

Below this parts of the section, there are taliks mainly lying under a layer of modern frozen strata. According to the shallow NTES data, they correspond to resistivity values from 5 to 10 Ω·m.

The lower layer of relict permafrost is located in the thickness of the Eocene-Paleocene deposits [Shatsky, 1978]. According to the shallow NTES data (Fig. 2), it corresponds to lower resistivity values, from 25 to 65 Ω·m, and its thickness presumably reaches 200 m. The deposits are represented by alternating layers of fine- and medium-grained sands, diatomite and opoka-like clays. Temperatures of –2...0 °C are typical for this depth interval [Ershov, 1989]. With depth, the temperature of the rocks relatively quickly rises to values at which phase transitions of water begin. However, due to the zero curtain effect, the rocks can remain in a frozen state for quite a long time [Baulin *et al.*, 1967; Shpolyanskaya, 1981; Ershov, 1989].



**Fig. 2.** Goelectric section along the profile surveyed by the shallow NTES method on the interfluvium between Khadutte and Tabykha rivers in their upper reaches.

1 – heaving mound; 2 – supposed bottom of the upper layer of modern permafrost; 3 – supposed bottom of the layer of frozen hydrate-bearing strata in the near-bottom part of modern permafrost; 4 – supposed base of the interpermafrost talik and the roof of the relict frozen rock; 5 – bottom of the lower relic layer of frozen rock; 6 – supposed accumulations of hydrate-bearing deposits; 7 – supposed channels of fluid migration. Q – Quaternary deposits, P<sub>2-3</sub> – Oligocene deposits, P<sub>2</sub> – Eocene deposits, and P<sub>1-2</sub> – Paleocene–Eocene deposits.

The anomalies in the form of high-resistivity pockets in the bottom part of the modern permafrost stratum identified according to the NTES data can probably be associated with both a local increase in the thickness of modern permafrost and the possible presence of hydrate-bearing deposits in the section [Misyurkeeva et al., 2017].

In accordance with the zoning map of the West Siberian oil and gas province [Kontorovich, 2008], the study area belongs to the Urengoy oil and gas field of the Nadym–Pur oil and gas region (OGR). At the same time, it is known that in the study area, at depths of 1100–1500 m, in the Cenomanian sediments, stage, there is a giant gas deposit. The Cenomanian productive stratum is characterized by significant heterogeneity. The most common in the section are fine-grained sandstones (sands) and siltstones (siltstones). Sandy-silty rocks are characterized by weak cementation. Sandstones and coarse-grained silts with kaolinite cement have good reservoir properties. The thickness of oil and gas reservoirs within the territory under consideration varies and is about 600–650 m. Spatial coincidence of the anomalies identified in the permafrost with the area of the predicted gas deposit in the Cenomanian strata (Fig. 3, d) is noted [Misyurkeeva et al., 2017].

Under the high-resistivity anomalies, in the underlying Eocene–Paleocene deposits (in the relic permafrost), subvertical anomalies of low resistivity relative to the host deposits are observed, which can probably be associated with gas migration channels (Fig. 2). A spatial coincidence of the areas of anomalies with the position of heaving mounds on the

earth’s surface was noted (Figs. 3, a, b, d), which may be indicative of the deep nature of the formation of these heaving mounds [Nezhdanov et al., 2011; Bogoyavlensky et al., 2019].

According to the totality of facts established during the shallow NTES work, namely: (1) the presence of high-resistivity “pockets” in the near-bottom part of the modern permafrost; (2) the presence of low resistivity anomalies on goelectric sections under the identified high-resistivity anomalies in the cryogenic stratum, interpreted as traces of fluid migration [Murzina et al., 2016; Misyurkeeva et al., 2017, 2021]; (3) the presence of heaving mounds on the surface associated with traces of deep fluid migration [Nezhdanov et al., 2011; Misyurkeeva et al., 2017, 2021; Bogoyavlensky et al., 2019] over the identified resistivity anomalies; and (4) the coincidence of goelectric anomalies and the areas of the predicted gas deposit in the Cenomanian sediments [Misyurkeeva et al., 2017], we can assume that the high-resistivity anomalies identified in the permafrost are associated with probable hydrate-containing deposits.

#### Evaluation of sensitivity of shallow NTES signals to identification of subpermafrost anomalies using mathematical modeling

To assess the sensitivity of nonstationary soundings to variations in the goelectric characteristics of permafrost (electrical resistivity and inductively induced polarization of rocks) and layers below it, mathematical modeling of induction transient characteristics was carried out. Its essence was to calculate the shallow NTES curves for the selected physi-



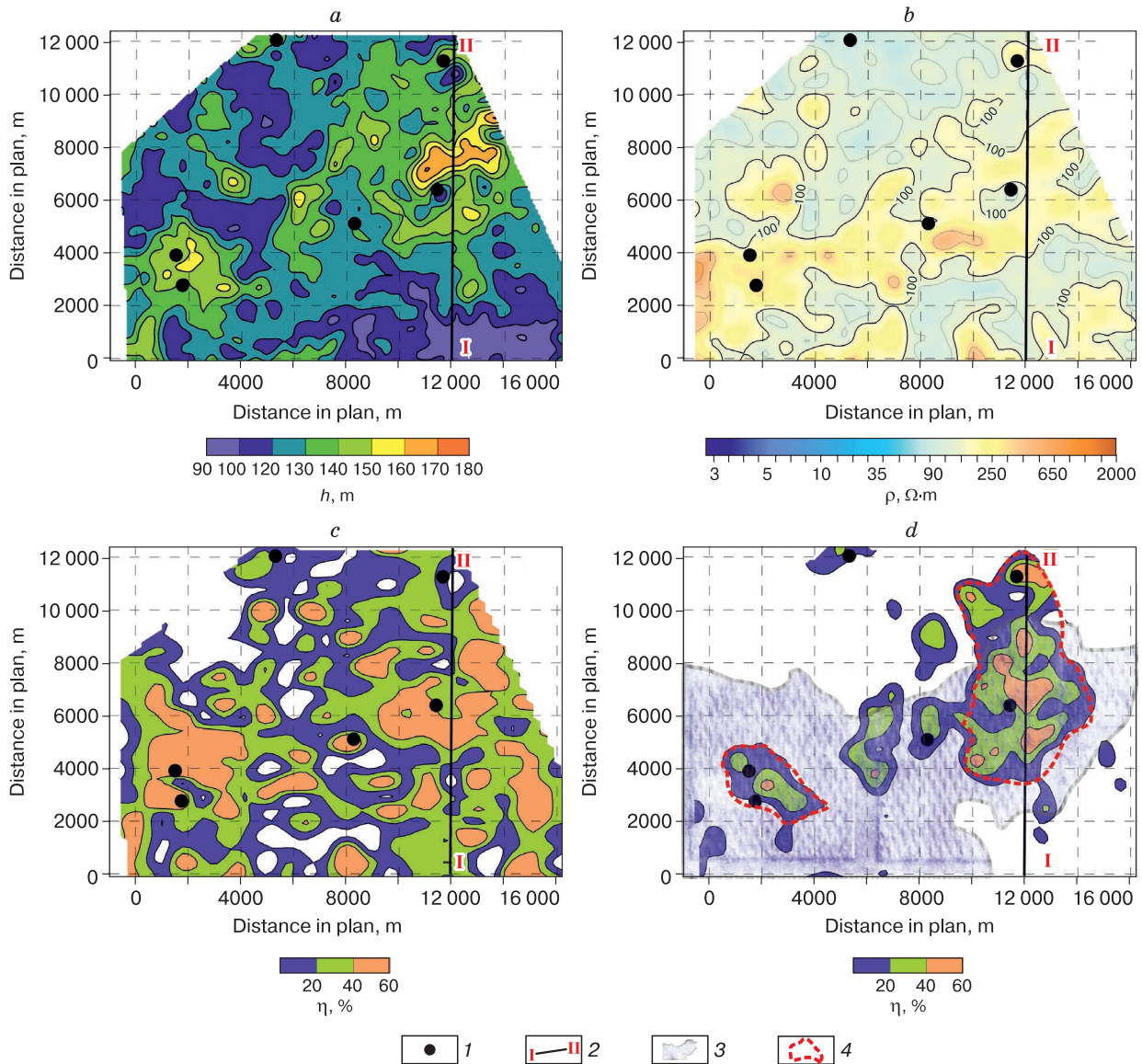


**Fig. 3. Results of shallow NTES data interpretation for the interfluvium between the Khadutte and Tabyakha rivers in their upper reaches.**

*a* – thickness map (*h*) of the upper modern permafrost, including the assumed layer of hydrate-bearing deposits (0–200 m); *b* – map of the normalized resistivity ( $\rho$ ) of the upper permafrost, including the assumed layer of hydrate-bearing deposits (0–200 m); *c* – map of the polarizability coefficient ( $\eta$ ) of the upper modern permafrost (0–90 m); *d* – map of the polarizability coefficient of the high-resistivity layer ( $\eta$ ) in the near-bottom part of the upper permafrost (90–200 m). 1 – heaving mound; 2 – position of the geoelectric profile; 3 – predicted area of gas field in the Cenomanian deposits; 4 – predicted area of hydrate-bearing deposits in the interpermafrost talik zone.

cal-geological model, apply electromagnetic (EM) interference characteristic of the area under study to them, and then solve the inverse problem of electrical exploration. When conducting a numerical experiment, calculations were carried out for an areal observation network using the shallow NTES method applied in the study.

Based on the results of interpretation of the shallow NTES data, simplified models  $M_1$  and  $M_2$  have

been developed. Model  $M_1$  is a standard model of permafrost, and model  $M_2$  is a model of permafrost with a lens of supposed hydrate-bearing deposits under the permafrost layer. These models formed the basis for further modeling (Table 1).

In the study area, layer 1 (the upper layer of modern permafrost) of a depth of 100 m is represented by ice-rich rocks with temperatures of about  $-5^\circ\text{C}$  and a resistivity of  $\rho = 2000 \Omega\cdot\text{m}$ . Permafrost polar-

ization parameters according to Kozhevnikov:  $\eta \approx 70\%$ ,  $\tau = 3 \cdot 10^{-5}$  s,  $C = 0.9$  [Kozhevnikov and Antonov, 2010].

Layer 2 lying directly below the icy frozen rocks, in which the existence of gas hydrates is assumed, is represented by sands with interlayers of siltstones, silty, micaceous and opoka-like clays. It is characterized by rather low resistivity values from 30 to 50  $\Omega$ -m. Temperatures of  $-4 \dots -2$   $^{\circ}\text{C}$  are typical for this depth interval, and the presence of pore ice is assumed, which is favorable conditions for both accumulation of gas hydrates and preservation of relict gas hydrates [Chuvilin et al., 2019].

If there are hydrate-containing deposits in the permafrost, then due to the absence of dissociation of crystallization water in gas hydrate molecules, their accumulation should have high resistivity. According to laboratory studies, the resistivity of gas hydrates is about 150  $\Omega$ -m [Permyakov et al., 2017]. Taking into account the heterogeneity of the studied geological objects, for a lens of hydrate-bearing deposits, the resistivity can be about 110–300  $\Omega$ -m. The manifestation of the FTI effect in the high-resistivity layer in the near-bottom part indicates the presence of ice in the lens. It is possible to assume that the polarization parameters of gas hydrates are similar to the properties of frozen rocks:  $\eta \approx 80\%$ ,  $\tau = 2 \cdot 10^{-4}$  s,  $C = 0.9$ . In the plantar part of the first and second layers, there is layer 3 (talik layer) with the average resistivity is 9  $\Omega$ -m. Below the taliks, there is a relic frozen strata (layer 4) characterized by low resistivity values of about 30  $\Omega$ -m. Its thickness is about 200 m.

The solution of direct and inverse problems within the framework of the accepted models  $M_1$  and  $M_2$  was carried out using the *Model 3* software [Aga-fonov et al., 2006]. The synthetic transient responses obtained in the framework of the model experiment were calculated up to a time of 10 ms. The duration of the synthetic transient characteristics calculated in

the framework of the model experiment was chosen based on the required depth of frozen strata (at least 400 m) and the geoelectric parameters of the given models. The first type of curve (Fig. 4) is characteristic of permafrost (Table 1,  $M_1$ ). The second type of curve (Fig. 4) is characteristic of permafrost in the presence of a high-resistivity body in the near-bottom part associated with a lens of hydrate-bearing deposits (Table 1,  $M_2$ ).

Several hundred responses were calculated, which were complicated by the addition of EM noise, in accordance with the noise parameters of real field data.

The area-averaged noise parameters were determined using the TEM-Processing software by processing a set of real noise records obtained with the FastSnap equipment [Sharlov et al., 2010] at one of the shallow NTES survey sites in Western Siberia [Sharlov et al., 2017]. Each noise record was a series of measured background values of electromagnetic noise (noise oscillogram with arithmetic time step) with the current turned off in the generator loop. To determine the maximum amplitude of the scatter of noise values (noise level), the noise record was recalculated into a logarithmic time grid corresponding to the time step of reading the synthetic curve. Next, the noise level was scaled to the level of the actually measured signal, i.e. normalization was performed for the value of current in the generator loop ( $I \sim 17\text{--}20$  A) and  $\sqrt[2]{N}$  where  $N$  is the number of accumulations performed when measuring real curves ( $N \sim 1600\text{--}2400$  accumulations). Figure 4 shows examples of synthetic responses calculated for different geoelec-

Table 1. Reference Models

Layer No.	$h$ , m	$\rho$ , $\Omega$ -m	$\eta$ , %	$\tau$ , s	$C$
<i>M<sub>1</sub>, geoelectric model of permafrost</i>					
1	100	2000	70	$3 \cdot 10^{-5}$	0.9
2	50	30	0	0	0
3	20	9	0	0	0
4	200	30	0	0	0
<i>M<sub>2</sub>, geoelectric model with a lens of hydrate-bearing sediments under the permafrost</i>					
1	100	2000	70	$3 \cdot 10^{-5}$	0.9
2	100	200	80	$2 \cdot 10^{-4}$	0.9
3	20	9	0	0	0
4	200	30	0	0	0

Note:  $h$  is layer thickness,  $\rho$  is the electrical resistivity,  $\eta$  is the polarizability coefficient,  $\tau$  is the relaxation time, and  $C$  is the degree of polarization.

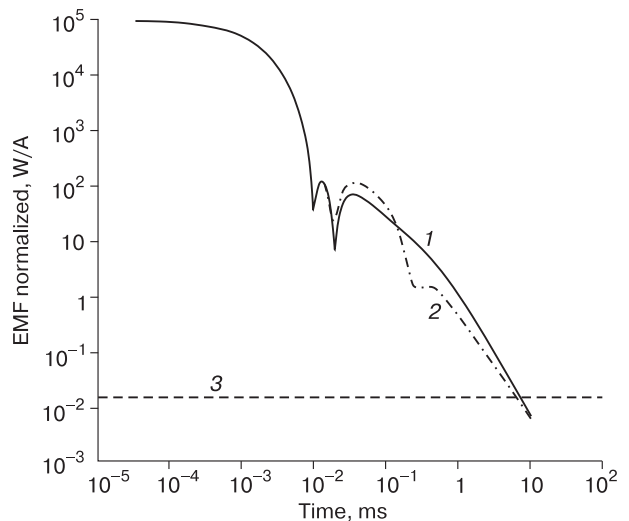


Fig. 4. Electromotive force (EMF) of the NTES signal vs time for models  $M_1$  and  $M_2$ .

1 – EMF curve for a coaxial loop over a polarized section of the frozen strata (Qq( $M_1$ )); 2 – EMF curve for a coaxial loop over a polarized section of the frozen strata with a lens of hydrate-bearing deposits (Qq( $M_2$ )); 3 – noise level.

Table 2. Models of subpermafrost anomaly associated with hydrate-containing deposits

No.	$\rho$ , %	$\eta$ , %	$h$ , m
1	10	20	35
2	20	30	40
3	30	40	45
4	40	50	50
5	50	55	60
6	60	60	70
7	70	65	75
8	80	70	85
9	90	80	90

Note:  $\rho$  – specific electrical resistance,  $\eta$  – polarizability coefficient,  $h$  – thickness.

tric conditions with a plotted noise level that does not exceed  $0.015 \mu\text{V}/\text{A}$ .

By interpolating the previously described reference models (Table 1), a three-dimensional geoelectric model of the geological section was formed with the presence of a gas hydrate deposit under the upper permafrost layer. The interpolation of the model took place in such a way that with each step, the analyzed subpermafrost layer was added 10 % of the resistivity parameters,  $\eta$  and  $h$  of the desired object (Table 2). The polarizability parameters were set for the first two horizons and for a subpermafrost high-resistivity object associated with gas hydrate accumulations. The relaxation time and the degree of polarization were fixed in accordance with the permafrost polar-

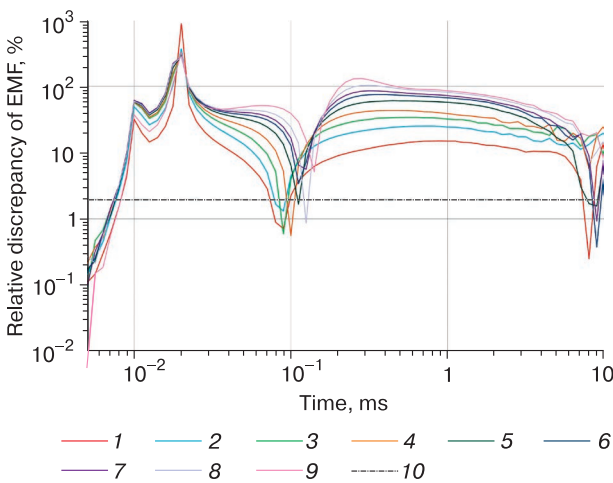


Fig. 5. Plot of relative discrepancy (%) between synthetic noisy EMF signals from the background model and the model with a successive increase in the anomalous contribution vs the relaxation time (Table 2).

1 to 9 – discrepancies between the synthetic curves of the shallow NTES in accordance with Table 2; 10 – the level of electromagnetic noise according to the actual field data.

ization indices according to N.O. Kozhevnikov [Kozhevnikov and Antonov, 2010].

On the graph of the percentage discrepancy (Fig. 5) between the coaxial shallow NTES curves calculated from the models obtained by changing the parameters (resistivity,  $\eta$ , and  $h$ ) of the subpermafrost layer, it can be seen that the amplitude of the anomaly is more than 100 % and repeatedly exceeds the noise level (2 %). This fact testifies to the high sensitivity of the NTES curves to changes in the subpermafrost conductive half-space.

Data inversion was carried out automatically using algorithms for solving poorly conditioned problems according to A.N. Tikhonov [Tikhonov and Arsenin, 1986]. A priori information was taken into account by fixing the number of layers in accordance with the geological model and the parameters of the first polarized permafrost layer. In the process of solving the inverse problem, it was necessary to establish the fact of a change in the geoelectric situation when a lens of hydrate-bearing deposits appeared under the permafrost.

Several cycles of inversion took place. Initially, the resistivity model and the thickness of the subpermafrost anomaly were determined. Then, the resistivity model and the anomaly thickness were refined with the selection of polarizability parameters. The logarithmic root-mean-square discrepancy between the practical and theoretical curves was used as the minimization functional, which tends to zero in the process of solving the inverse problem.

When the discrepancy was less than 3 %, the sensitivity of the sounding curves to the electromagnetic anomaly was estimated. To do this, the root-mean-square error  $\delta$ , % (Table 3) of the desired parameters was calculated for the groups of curves formed in accordance with Table 2.

Table 3. Results of synthetic modeling of shallow NTES signals

No.	Root-mean-square error of reconstruction of an anomalous object parameters		
	$\delta_{\text{SER}}$ , %	$\delta_{\eta}$ , %	$\Delta_h$ , %
1	31	43	9
2	27	40	9
3	22	30	5
4	16	20	5
5	10	25	10
6	11	17	13
7	11	7	13
8	6	5	2
9	10	1	5

Note:  $\delta_{\text{SER}}$  is the rms error in determining the electrical resistivity,  $\delta_{\eta}$  is the rms error in determining the polarizability coefficient,  $\Delta_h$  is the rms error in determining the thickness.



Based on the results of modeling the shallow NTES curves for the southern part of the Tazovsky Peninsula (the area between the Khadutte and Tabyakha rivers), it is possible to confidently identify high-resistivity anomalies with a relative value of 40 % with accompanying anomalies  $\eta \sim 50$  % and the anomaly thickness increase by more than 50 m.

### CONCLUSIONS

The features of the geoelectric section of permafrost identified from data of near-field transient electromagnetic sounding at the key site in Nadym district of the Yamalo-Nenets Autonomous okrug, on the interfluvium between the Khadutte and Tabyakha rivers in their upper reaches, allow us to draw the following conclusions:

- high-resistivity resistivity SER anomalies obtained from the NTES field experiment and accompanied by DIP anomalies can be associated with changes in the permafrost structure, as well as with the possibility of the existence of gas hydrates in the cryogenic layer;

- the coincidence of the spatial position of gas fields in the deposits of the Cenomanian stage and the anomalies identified according to the NTES data in the near-surface part of the section may indicate the possible deep nature of the formation of gas hydrate accumulations in the permafrost;

- subvertical anomalies of low SER under high-resistivity anomalies can characterize manifestations of deep fluid migration;

- according to NTES, in the geological section of the northern part of Western Siberia, one can confidently identify subpermafrost anomalies of increased SER with a relative value of 40 % accompanied by anomalies  $\eta \sim 50$  % with an increase in the thickness by more than 50 m;

- it is advisable to recommend a drilling study of the identified geophysical anomalies to clarify their nature and assess their possible connection with gas hydrate deposits.

**Acknowledgments.** *The authors are grateful to the General Director of SIGMA-GEO LLC, Cand. Sci. Yu.A. Agafonov for the opportunity to use the materials. The authors are grateful to Prof. Dr. Sci. N.O. Kozhevnikov for help in shaping the structure of the article and constructive suggestions. We also thank Cand. Sci. V.E. Tumskoy and Cand. Sci. E.M. Chuvilin for their invaluable help in the preparation of the final version of the article and highly appreciate fair criticism of the reviewers, which made it possible to significantly improve the final text.*

### References

- Agafonov, Yu.A., Pospeev, A.V., Surov, L.V., 2006. The system of data interpretation and main directions of application of the results of nonstationary electromagnetic sounding to the south of Siberian Craton. *Pribery Sistemy Razvedochn. Geofiziki*, No. 1, 33–36 (in Russian).
- Ageev, D.V., 2019. Application of nonstationary electromagnetic sounding for solving hydrogeological problems in the permafrost zone of the Novyi Urengoy oil and gas field. *Inzhenern. Izyskaniya* XIII (3), 40–47 (in Russian).
- Afanasenkov, A.P., Volkov, R.P., Yakovlev, D.V., 2015. Increased electric resistivity anomaly under permafrost sediments layer as a new indicator for prospecting hydrocarbon deposit. *Geol. Nefti Gaza*, No. 6, 40–51 (in Russian).
- Aregbe, A.G., 2017. Gas hydrate – properties, formation and benefit. *Open J. Yangtze Oil and Gas*, 2 (1), 27–44.
- Baulin, V.V., Belopukhova, E.B., Dubikov, G.I., Shmelev, L.M., 1967. *Geocryological Conditions of the West Siberian Lowland*. Moscow: Nauka, 213 p. (in Russian).
- Bogoyavlensky, V.I., Sizov, O.S., Mazharov, A. et al., 2019. Earth degassing in the Arctic: remote and field studies of the Seyakha catastrophic gas blowout on the Yamal Peninsula. *Arktika: Ekologiya Ekonomika*, No. 1 (33), 88–105 (in Russian). doi: 10.25283/2223-4594-2019-1-88-105.
- Bondarev, V.L., Mirotvorskii, M.Yu., Shaidullin, R.M., Gudzenko, V.T., 2004. Conditions for the Formation of Nonindustrial Hydrocarbon Gas Accumulations in the Supraproductive Deposits of the Yamal Peninsula and Geochemical Methods for Diagnosing Their Nature. Moscow: NPC “Geokhimiya” – Nadymgazprom, 182 p. (in Russian).
- Bondarev, V.L., Mirotvorskii, M.Yu., Zvereva, V.B. et al., 2008. Gas geochemical characteristics of the supra-Cenomanian deposits of the Yamal Peninsula (on the example of the Bovanenkovo oil condensate field). *Geol. Geofizika Razrabotka Neftyan. Gazovykh Mestorozhdenii*, No. 5, 22–34 (in Russian).
- Buddo, I.V., Misurkeeva, N.V., Shelohov, I.A. et al., 2017. Experience of 3D transient electromagnetics application for shallow and hydrocarbon exploration within Western Siberia. In: *Proc. 79<sup>th</sup> EAGE Conf. Exhibition 2017* (Paris, France, 12–15 June 2017). doi: 10.3997/2214-4609.201700667.
- Buddo, I.V., Smirnov, A.S., Misurkeeva, N.V. et al., 2018. Integration of electromagnetic and seismic survey data at all stages of geological exploration: from the prospecting stage to the development of hydrocarbon fields. *Ekspozitsiya Neft’ Gaz* October, No. 6 (66), 24–28 (in Russian).
- Buddo, I.V., Seminskij, I.K., Shelohov, I.A. et al., 2021. Electromagnetic studies for cryolithozone investigation in the Arctic settings: background of application and experimental data. In: *Proc. Conf. “Modern Studies of Cryosphere Transformation and Issues of Geotechnical Safety of Structures in the Arctic”*. V.P. Melnikov and M.R. Sadurtdinov (Eds.). Salekhard, p. 71–74 (in Russian).
- Chersky, N.V., Tsarev, V.P., 1973. Prospects for the Development of Gas Hydrate Deposits. Research and Recommendations for Improving Mining in the Northern and Eastern Regions of the USSR, Part 1. Yakutsk: Izd. Yakutskogo Filiala Sib. Otd. Akad. Nauk SSSR, 121 p. (in Russian).
- Chuvilin, E., Bukhanov, B., Davletshina, D. et al., 2018. Dissociation and self-preservation of gas hydrates in permafrost. *Geosciences* 8, 431 p. doi: 10.3390/geosciences8120431.
- Chuvilin, E.M., Davletshina, D.A., Lupachik, M.V., 2019. Hydrate formation in frozen and thawing methane-saturated sediments. *Earth’s Cryosphere*, XXIII (2), 44–52.
- Chuvilin, E.M., Perlova, E.V., Baranov, Yu.B. et al., 2007. Structure and Properties of Permafrost in the Southern Part of the Bovanenkovo Gas Condensate Field. Moscow: GEOS, 135 p. (in Russian).



- Chuvilin, E.M., Yakushev, V.S., Perlova, E.V., 2000. Gas and gas hydrates in the permafrost of Bovanenkov gas field, Yamal Peninsula, West Siberia. *Polarforschung* **68**, 215–219.
- Dolgikh, Y., Sanin, S., Buddo, I. et al., 2019. Improving the efficiency of geophysical research based on the integration of seismic and modern electrical exploration. In: Proc. Conf. Tyumen 2019 (March 2019). Vol. 1, p. 1–5. doi: <https://doi.org/10.3997/2214-4609.201900577>.
- Ershov, E.D., 1989. Geocryology of the USSR. Western Siberia. Moscow: Nedra, 454 p. (in Russian).
- Istomin, V.A., Yakushev, V.S., 1992. Gas Hydrates in Natural Conditions. Moscow: Nedra, 236 p. (in Russian).
- Kontorovich, A.E., 2008. Geology of Oil and Gas. Selected Works. Vol. 1. Geology of Oil and Gas in Siberia. Novosibirsk: Izd. SNIIGTMS, 540 p. (in Russian).
- Kozhevnikov, N.O., Antonov, E.Yu., 2010. Inversion of IP-affected NTES responses of a two-layer earth. *Russian Geology and Geophysics* **51** (6), 905–918.
- Kozhevnikov, N.O., Antonov, E.Yu., Zaharkin, M.A. et al., 2014. NTES surveys for search of taliks in areas of strong fast-decaying IP effects. *Russian Geol. Geophysics* **55** (12), 1815–1827.
- Leonov, S.A., 2010. Prospects for the hydration potential of the supra-Cenomanian deposits in the north of Western Siberia. Author's abstract Cand. Sci. diss. Moscow, 24 p. (in Russian)
- Misyurkeeva, N.V., Buddo, I.V., Agafonov, Yu.A. et al., 2017. Shallow NTES and NTES electromagnetic studies application in geological settings of Arctic zone of Western Siberia. In: Proc. Conf. Geomodel 2017 (Gelendzhik, Russia, Sept. 11–14, 2017) (in Russian). doi: [10.3997/2214-4609.201702225](https://doi.org/10.3997/2214-4609.201702225).
- Misyurkeeva, N.V., Buddo, I.V., Sholokhov, I.A. et al., 2021. Permafrost structure in the north of Western Siberia from modern geophysical studies. In: Proc. Int. Conf. “Modern Studies of Cryosphere Transformation and Issues of Geotechnical Safety of Structures in the Arctic”. V.P. Melnikov and M.R. Sadurtdinov (Eds.). Salekhard, p. 297–300 (in Russian).
- Misyurkeeva, N.V., Buddo, I.V., Shelohov, I.A. et al., 2019. New data on fluid dynamic processes in the Arctic Zone of Western Siberia based on the results of TEM, STEM electromagnetic studies and seismic CDP studies. In: Proc. Conf. Tyumen 2019 (March 2019), p. 1–6. doi: [10.3997/2214-4609.201900574](https://doi.org/10.3997/2214-4609.201900574)
- Misyurkeeva, N.V., Buddo, I.V., Smirnov, A.S. et al., 2020. Shallow transient electromagnetic method application to study the Yamal Peninsula permafrost zone. In: Proc. Conf. Geomodel 2020 (Gelendzhik, Russia, Sept. 2020). Vol. 2020, p. 1–6. doi: [10.3997/2214-4609.202050105](https://doi.org/10.3997/2214-4609.202050105)
- Murzina, E.V., Misyurkeeva, N.V., Buddo, I.V. et al., 2016. The result of the application of automatic inversion for permafrost studies using high-density NTES soundings. In: Proc. 13<sup>th</sup> Sci. Practical Seminar “Application of Modern Electric Exploration Technology in Prospecting Mineral Deposits” (Saint Petersburg, Nov., 2016), p. 119–122 (in Russian).
- Nezhdanov, A.A., Novopashin, V.F., Ogibenin, V.V. et al., 2011. Mud volcanism in the north of Western Siberia. Tr. Inst. TyumenNIIGiprogaz: Geolog. Geologorazvedka. Tyumen: Flat, p. 73–79 (in Russian).
- Perlova, E.V., 2001. Features of Gas Content in Permafrost by the Example of the Northwestern Part of Yamal Peninsula. Cand. Sci. (Geol.-Mineral.) diss., Moscow, 174 p. (in Russian).
- Perlova, E.V., Miklyaeva, E.S., Leonov, S.A. et al., 2017. Gas hydrates of the Yamal Peninsula and adjacent shelf of the Kara Sea as a complicating factor in the development of the region. *Problemy Resursn. Obespecheniya Gazodobyv. Raionov Rossii*, No. 3 (**31**), 255–262 (in Russian).
- Permyakov, M.E., Manchenko, N.A., Duchkov, A.D. et al., 2017. Laboratory modeling and measurement of the electrical resistivity of hydrate-bearing sand samples. *Geol. Geophysics* **58** (5), 792–800.
- Romanovskiy, N.N., 1993. Foundations of Lithosphere Cryogenesis. Moscow: Izd. Mosk. Gos. Univ., 336 p. (in Russian).
- Rybalchenko, V.V., Trusov, A.I., Buddo, I.V., et al., 2020. A complex of auxiliary studies at the stages of exploration and development of oil and gas fields: from mapping permafrost to prospecting for groundwater to ensure drilling and operation. *Gazovaya Promyshlennost*, No. 11 (808), 20–28 (in Russian).
- Sharlov, M.V., Agafonov, Yu.A., Stefanenko, S.M., 2010. The modern telemetric electric exploration stations “SGS-TEM” and “FastSnap”. Efficiency and experience of use. *Priboiy i Sistemy Razvedochnoi Geofiziki (Saratov)*, No. 1 (**31**), 20–24 (in Russian).
- Sharlov, M.V., Buddo, I.V., Misyurkeeva, N.V. et al., 2017. Transient electromagnetic surveys for high resolution near-surface exploration: basics and case studies. *First Break* **35** (9), 63–71.
- Shatsky, S.B., 1978. Paleogene and Neogene of Siberia. Novosibirsk: Nauka, 168 p. (in Russian).
- Shelokhov, I.A., Buddo, I.V., Smirnov, A.S. et al., 2018. Inversion of TEM responses to create a near surface velocity structure. *First Break* **36** (10), 47–51. doi: [10.3997/1365-2397.n0125](https://doi.org/10.3997/1365-2397.n0125).
- Shpolyanskaya, N.A., 1981. Frozen zone of the Lithosphere of Western Siberia and Tendency of Its Development. Moscow: Izd. Mosk. Gos. Univ., 167 p. (in Russian).
- Stogniy, V.V., 2003. Pulsed Inductive Electrical Exploration of Permafrost Taliks in Central Yakutia. Yakutsk, 124 p. (in Russian).
- Tikhonov, A.N., Arsenin, V.Ya., 1986. Methods for Solving Ill-Posed Problems. Moscow: Nauka, 286 p. (in Russian).
- Uchida, T., Dallimore, S., Mikati, J., 2000. Occurrences of natural gas hydrates beneath permafrost zone in Mackenzie delta: visual and X-ray imaginary. *Ann. New York Acad. Sci.* **912**, 1021–1033.
- Vanyan, L.L., 1965. Fundamentals of Electromagnetic Sounding. Moscow: Nedra, 109 p. (in Russian).
- Vorob'ev, A.E., Malyukov, V.P., 2009. Gas Hydrates. The impact of Technology on Unconventional Hydrocarbons. Moscow: Izd. RUDN, 289 p. (in Russian).
- Yakushev, V.S., 2009. Natural Gas and Gas Hydrates in the Cryolithozone. Moscow: VNIIGAZ, 192 p. (in Russian).
- Yakushev, V.S., Chuvilin, E.M., 2000. Natural gas and hydrate accumulation within permafrost in Russia. *Cold Reg. Sci. Technol.* **31**, 189–197.
- Yakushev, V.S., Perlova, E.V., Makhonina, N.A. et al., 2003. Gas hydrates in sediments of continents and islands. *Russ. Khimich. Zh.* **XLVII** (3), 80–90 (in Russian).

Received September 16, 2019

Revised December 17, 2021

Accepted February 28, 2022

Translated by A.V. Muravyov